Published in final edited form as:
Sci Signal. ; 3(153): ra91. doi:10.1126/scisignal.2001423.

CYCLIC GMP/PROTEIN KINASE G CONTROL A SRC-CONTAINING MECHANOSOME IN OSTEOBLASTS

Hema Rangaswami[1], **Raphaela Schwappacher**[1], **Nisha Marathe**[1], **Shunhui Zhuang**[1], **Darren E. Casteel**[1], **Bodo Haas**[2], **Yong Chen**[2], **Alexander Pfeifer**[2], **Hisashi Kato**[1], **Sanford Shattil**[1], **Gerry R. Boss**[1], and **Renate B. Pilz**[1,*]

[1] Department of Medicine, University of California San Diego, La Jolla, CA 92093, USA

[2] Institute for Pharmacology and Toxicology, University of Bonn, 53105 Bonn, Germany

Abstract

Mechanical stimulation is crucial for bone growth/remodeling, and fluid shear stress promotes anabolic responses in osteoblasts through multiple second messengers, including nitric oxide (NO), but the underlying mechanisms are not well understood. Here we demonstrate that the NO/cGMP/PKG signaling pathway activates Src in mechanically-stimulated osteoblasts, initiating a proliferative response. PKG II is necessary for Src activation, which also requires Src docking to β_3 integrins and Src dephosphorylation by a Shp-1/2 phosphatase complex. PKG II directly phosphorylates and stimulates Shp-1 activity, and fluid shear stress triggers PKG II, Src, and Shp recruitment to a mechanosome containing β_3 integrins. PKG II-null mice show defective osteoblast Src/Erk signaling, and decreased Erk-dependent gene expression in bone. Our findings reveal crosstalk between NO/cGMP/PKG and integrin signaling and establish a new mechanism of Src activation. Since Src controls Erk, which is key to osteoblast growth and survival, these results support use of PKG-activating drugs as mechano-mimetics for treating osteoporosis.

INTRODUCTION

Mechanical stimulation induces bone growth and remodeling, which is critical for maintaining bone mass and strength (1). Compressive forces generated by weight bearing and locomotion induce small bone deformations and increase interstitial fluid flow; in response to these mechanical stimuli, osteoblasts lining endosteal and periosteal surfaces proliferate and differentiate, and osteocytes embedded in the canalicular bone network show enhanced survival (1,2). Mechanoreceptors on osteoblasts and osteocytes include integrins associated with cytoskeletal proteins, and mechano-sensitive calcium channels (2). Mechanical stimulation rapidly and transiently increases intracellular calcium, and NO and prostaglandin E2 production (3,4). These second messengers activate various signal transduction pathways, e.g. the Raf/MEK/Erk1/2 cascade, leading to changes in gene expression (3).

*Corresponding author (rpilz@ucsd.edu).

Author contributions: H.R. performed BrdU uptake, fluid shear- and cGMP induced Src/Erk phosphorylation, siRNA and viral reconstitution experiments, and with N.M. isolated hPOBs and performed RT-PCR. R.S. carried out the interaction and colocalization studies. S.Z. and D.E.C. performed site-directed mutagenesis, PTP activity and phosphorylation studies. B.H., Y.C., and A.P. generated PKG II-deficient mice and isolated mPOBs,. H.K. prepared β_3 integrin virus. R.B.P, H.R. R.S., G.R.B., and S.S. designed experiments, analyzed data, and wrote the manuscript.

Competing interests: The authors declare no conflicts of interest.

NO synthesis in mechanically-stimulated osteoblasts and osteocytes occurs, in part, through activation of endothelial NO synthase (eNOS) and increased inducible NOS (iNOS) expression (5,6). NO is important for bone (re)modeling, as evidenced by in vitro and in vivo studies: (i) low doses of NO donors promote osteoblast proliferation and differentiation in vitro, and increase bone formation in response to mechanical stimulation (7,8); (ii) young eNOS-deficient mice have reduced bone mass due to defects in osteoblast number and maturation, and adults show impaired bone adaptation to interstitial fluid flow (9,10); and (iii) iNOS-deficient mice and rodents treated with NOS inhibitors fail to increase bone formation after mechanical stimulation (6,11,7).

NO produced in mechanically-stimulated osteoblasts and osteocytes activates soluble guanylate cyclase, increasing intracellular cGMP, which activates both soluble type I and membrane-bound type II PKG; other cGMP targets include phosphodiesterases and cyclic nucleotide-gated ion channels (5,12). PKG II-deficient mice are dwarfs due to a block in chondrocyte differentiation in bone growth plates, while PKG I-deficient mice have no obvious skeletal abnormalities (13). We recently demonstrated that NO/cGMP cooperate with a calcium-dependent pathway to activate Erk in response to fluid shear stress, but the mechanism(s) whereby shear stress activates Erk are largely unknown (5). Here, we establish a new signaling pathway of NO/cGMP/PKG II activating Erk via Shp-1/2 and Src in shear-stressed osteoblasts, and show defective signaling in PKG II-deficient mice. We uncover a missing link between NO/cGMP/PKG and β_3 integrins explaining the requirement of both pathways for Erk activation in osteoblasts and osteocytes.

RESULTS

PKG II is Necessary for Fluid Shear Stress -induced Osteoblast Proliferation

Fluid shear stress stimulates osteoblast proliferation in an Erk-dependent fashion (14,15), and this in vitro response correlates well with increased bone formation during mechanical stimulation in vivo, based on the differential osteogenic response to mechanical stress in different inbred strains of mice (16). Since we previously showed that the NO/cGMP/PKG II signaling pathway is necessary for fluid shear stress-induced Erk activation (5), we examined the role of PKG II in early osteoblast proliferation using an siRNA approach. We found that 15 min of laminar fluid shear stress (at 12 dynes/cm^2) stimulated bromo-deoxyuridine (BrdU) uptake into replicating DNA by ~three-fold in MC3T3-E1 murine osteoblast-like cells (referred to as MC3T3), and siRNA-mediated depletion of PKG II prevented this response (Fig. 1, A and B; PKG II depletion is shown in Suppl. fig. S1A). Treatment with 8-(4-chlorophenylthio)-guanosine-3′,5′-cyclic monophosphate (8-CPT-cGMP; referred to as cGMP) mimicked the effects of fluid shear stress on cell proliferation in cells transfected with an siRNA targeting green fluorescent protein (GFP), but had no effect in PKG II siRNA-transfected cells (Fig. 1, A and B). Thus, PKG II activity is required for shear- and cGMP-induced early osteoblast proliferation. However, fluid shear responses may vary with the degree of osteoblast differentiation (1).

Fluid Shear Stress- or cGMP-induced Erk Activation Requires Src

Src activity is regulated by phosphorylation: in resting cells, the C-terminal Tyr^{529} is phosphorylated and interacts with the SH2 domain keeping Src in a “closed” (inactive) conformation; dephosphorylation of Tyr^{529} is a key event in Src activation, changing the protein to an “open” conformation and allowing auto-phosphorylation of Tyr^{418} in the kinase domain activation loop (Fig. 1C) (17). Exposing primary human osteoblasts (hPOBs), murine MC3T3 osteoblast-like cells, and MLO-Y4 osteocyte-like cells to fluid shear stress for up to 30 min rapidly induced Src dephosphorylation on Tyr^{529} and phosphorylation on Tyr^{418}, indicating Src activation. Src activation peaked slightly before Erk activation, and

treating cells with an NO donor or cGMP mimicked the effects of fluid shear stress [Fig. 1, D to F, and fig. S1, B to D; please note that results obtained with antibodies specific for Src with Tyr^{529} phosphorylated (Src-pTyr^{529}) or unphosphorylated (Src-nonpTyr^{529}) are mirror images of each other].

The Src family kinase inhibitor PP2 prevented fluid shear stress-induced Src auto-phosphorylation and Erk activation, but the inactive analog PP3 was without effect; similarly, PP2, but not PP3 prevented cGMP-induced Erk activation (Fig. 1, G and H, and fig. S1E). siRNA-mediated Src knockdown blocked fluid shear stress- and cGMP-induced Erk-1/2 activation, while a control siRNA had no effect (Fig. 1, I and J, and fig. S1F). Thus, Src is required for Erk activation in fluid shear stress- or cGMP-stimulated osteoblasts.

Membrane-localized PKG Mediates Src Activation

To determine whether fluid shear stress-induced Src activation was mediated by the NO/cGMP/PKG pathway, we used pharmacologic inhibitors of NOS (L-NAME), soluble guanylate cyclase (ODQ), and PKG (Rp-8-CPT-PET-cGMPS, abbreviated Rp) (Fig. 2A). Each of these agents almost completely prevented fluid shear stress-induced Src Tyr^{418} auto-phosphorylation and Tyr^{529} dephosphorylation in hPOBs and MC3T3 cells (Fig. 2, B and C). Thus, fluid shear stress-induced Src activation requires NO/cGMP/PKG signaling. To determine which PKG isoform mediated Src activation, we used siRNAs to selectively deplete cytosolic PKG I or membrane-bound PKG II (fig. S1A). siRNA-mediated knockdown of PKG II completely prevented fluid shear stress- and cGMP-induced Src activation, whereas PKG I knockdown was without effect (Fig. 2D).

To assess whether the differing ability of PKG I and II to regulate Src activity was due to differences in subcellular localization and/or substrate recognition, we reconstituted PKG II-depleted MC3T3 cells with siRNA-resistant PKG constructs. Wild-type PKG II expressed in PKG II-deficient cells restored cGMP-induced Src activation, but similar amounts of a membrane binding-deficient PKG II-G2A mutant did not (Fig. 2, E to G); the mutant PKG II-G2A is cytosolic because it lacks the N-terminal myristoylation signal that targets PKG II to the plasma membrane (18). A membrane-targeted PKG I/II chimera containing the N-terminal 39 amino acids of PKG II fused to the N-terminus of PKG I (PKG I-swap) restored cGMP-induced Src activation in PKG II siRNA-treated MC3T3 cells, whereas similar amounts of wild-type PKG I did not (Fig. 2, E to G). All four PKG constructs produce similar total cellular PKG activities, but in different subcellular compartments (18). We conclude that membrane-targeting of PKG activity is essential for cGMP-induced Src activation, and that it involves a substrate recognized by both PKG I and II.

Src is Not Directly Activated by PKG II

cAMP-dependent protein kinase (PKA) activates Src directly by phosphorylating Ser^{17}, a site that could potentially be recognized by PKG (19). Purified PKG II did not affect Src (auto)phosphorylation and did not phosphorylate the PKA recognition site(s) in Src under conditions where a known PKG/PKA substrate was efficiently phosphorylated (fig. S2, A to C). Some phosphorylation of the PKA recognition site(s) in Src was detectable in untreated MC3T3 cells; this phosphorylation was not increased in cGMP-treated cells, but was increased when PKA was activated with 8-Br-cAMP (fig. S2D). Thus, Src is not a PKG II substrate, and is not activated by direct PKG II phosphorylation or interaction with PKG II.

Fluid Shear Stress- and cGMP-induced Src Activation is Mediated by Shp-1/2

Rapid dephosphorylation of Src pTyr^{529} in fluid shear stress- or cGMP-treated osteoblasts (Fig. 1, D to F) implies involvement of (a) protein tyrosine phosphatase(s) (PTP). The PTP inhibitor vanadate did not affect Src phosphorylation at Tyr^{529} in resting osteoblasts,

indicating low activity of PTPs which catalyze Src pTyr^{529} dephosphorylation. However, vanadate completely blocked fluid shear stress- and cGMP-induced Src pTyr^{529} dephosphorylation and prevented Src Tyr^{418} auto-phosphorylation (Fig. 3, A and B, and fig. S3A). These results suggest PKG regulates Src via activation and/or recruitment of PTP(s) catalyzing Src pTyr^{529} dephosphorylation.

Osteoblasts express several PTPs which can dephosphorylate Src Tyr^{529} *in vitro*, including the tandem SH2 domain-containing PTPs Shp-1 and -2, PTP-1B, and the receptor-type phosphatase RPTP-α. All four proteins contain potential PKG phosphorylation sites and may activate Src in intact cells (20,21). Depleting either Shp-1 or Shp-2 by siRNAs prevented fluid shear stress- and cGMP-induced Src pTyr^{529} dephosphorylation in MC3T3 cells, whereas depleting PTP-1B or PTP-α had no effect (Fig. 3D and fig. S3, B and C; efficient and specific knockdown of target proteins is shown in Fig. 3C). Reconstitution of siRNA-resistant human Shp-1 or -2 in Shp-1 or -2-depleted MC3T3 cells fully restored cGMP-induced Src pTyr^{529} dephosphorylation and Tyr^{418} auto-phosphorylation as well as Erk activation (Fig. 3, E and F). Depletion and reconstitution of Shp-1 did not affect Shp-2 amounts (and vice versa). These results indicate that Shp-1 and -2 are both required for fluid shear stress- and cGMP-induced Src activation. Shp-1 and -2 also co-operate in epidermal growth factor-induced Erk activation, with Shp-2 acting as a scaffold recruiting Shp-1 to the receptor (22).

PKG II Phosphorylates Shp-1 and Stimulates PTP Activity

Shp-1 and -2 phosphatase activities are regulated by interactions between their respective SH2 and PTP domains, and by phosphorylation of Tyr in the C-terminal tail, where the sequences of the two phosphatases diverge the most (21). We found that PKG II strongly phosphorylated purified full-length Shp-1 wild-type (WT) and N- terminally truncated Shp-1 (ΔSH2, missing the two SH2 domains), but not the isolated catalytic domain (CAT); this localized the PKG phosphorylation site(s) to the C-terminal tail (Fig. 4, A and B). Under similar conditions, Shp-2 was not efficiently phosphorylated.

We measured Shp-1 phosphatase activity using a pTyr^{529}-containing Src peptide as a substrate. The specific activity of purified Shp-1ΔSH2 was similar to that of the isolated catalytic domain (CAT) and ~5-fold higher than that of the full-length enzyme (Fig. 4C), consistent with results reported for other substrates (21). PKG II phosphorylation of full-length Shp-1 or Shp-1ΔSH2 stimulated phosphatase activity, but PKG II did not stimulate Shp-1 CAT activity (Fig. 4C). Thus, PKG II phosphorylation of the Shp-1 C-terminal tail stimulates Shp-1 PTP activity towards Src pTyr^{529} in vitro.

Phosphorylation of Flag-tagged, full-length Shp-1 in 293T cells was enhanced by wild-type, but not kinase-dead PKG II, and Shp-1 phosphorylation occurred on serine(s) (Fig. 4D and fig. S4A). A Shp-1 construct lacking the C-terminal 74 amino acids (Shp-1ΔCT) showed neither basal nor PKG II-stimulated phosphorylation, and a construct containing alanines substituted for Ser^{553}, Ser^{556}, and Ser^{557} in a potential PKG recognition sequence (Shp-1AAA) showed reduced basal phosphorylation with minimal change in the presence of PKG II (Fig. 4E). Thus, PKG II targets at least one of these serines, which are highly conserved among species but not present in Shp-2 (fig. S4B). Flag-Shp-1 isolated from 293T cells expressing wild-type PKG II had about two-fold more PTP activity than Shp-1 from cells co-transfected with empty vector or kinase-dead PKG II; in these experiments, wild-type PKG II expression did not alter the amount of Flag-Shp-1 protein in the cell. The PTP activities of Shp-1ΔCT and Shp-1AAA were not affected by PKG II, consistent with their lack of PKG phosphorylation (Fig. 4F). In contrast to wild-type Shp-1, which restored cGMP-induced Src activation in Shp-1-siRNA-treated MC3T3 cells, Shp-1ΔCT or

Shp-1AAA were ineffective (Fig. 4G). Thus, Shp-1 phosphorylation and activation by PKG II is necessary for Src activation.

Shp-1-specific antibodies did not immunoprecipitate sufficient Shp-1 from MC3T3 cells to measure PTP activity; however, we found that Shp-1 co-immunoprecipitated with Shp-2 (Fig. 4H), consistent with direct binding of the two proteins (22). We used Shp-2 antibodies to isolate a complex of endogenous Shp-1 and -2 from MC3T3 cells and found that cGMP stimulated PTP activity (Fig. 4I and fig. S4C). cGMP stimulation neither altered the proportion of Shp-1 and Shp-2 in the complex (Fig. 4H) nor affected Tyr phosphorylation of endogenous Shp-1/2 (fig. S4D).

Src and Erk Activation by cGMP/PKG II Requires $\alpha_v\beta_3$Integrin Ligation

Integrins link extracellular matrix proteins to the actin cytoskeleton, and anchoring of integrins to actin stress fibers is essential for fluid shear-induced *c-fos* induction (23). Osteoblasts express several integrins, including $\alpha_v\beta_3$ (2). Erk activation in fluid shear- or stretch-stimulated osteoblasts is prevented by β_3-blocking antibodies and siRNA-mediated knockdown of β_3 (24,25). We found that siRNA depletion of β_3 prevented cGMP-induced Src and Erk activation in MC3T3 cells (Fig. 5, A and B). The siRNAs did not affect β_1 expression or MC3T3 cell adhesion, the latter likely because cells adhere to secreted extracellular matrix proteins via multiple integrins. cGMP-induced Src and Erk activation were restored by expressing siRNA-resistant human β_3 in β_3-depleted cells, but not by a $\beta_3\Delta$CT mutant that does not bind Src [Fig. 5, C and D; $\beta_3\Delta$CT lacks the last three C-terminal amino acids (26)]. Thus, Src activation by PKG II requires Src interaction with the cytoplasmic tail of β_3.

To determine whether cGMP/PKG II activation of Src and Erk requires ligand binding to β_3 integrins, osteoblasts were placed either in suspension, or allowed to adhere to fibrinogen-coated plates for 1 hour (fibrinogen was used as a specific ligand for integrin $\alpha_v\beta_3$, and waiting 1 hour assured that Erk activation during cell spreading had subsided). cGMP activated Src and Erk in cells plated on fibrinogen (FB), but had no effect on suspension cells, unless $MnCl_2$ was added to directly activate $\alpha_v\beta_3$ and enable soluble fibrinogen binding (Fig. 5E and and fig. S5). Similar results were obtained with fibronectin (FN, fig. S5). Thus, cGMP/PKG II activation of Src and Erk in osteoblasts requires adhesive ligand (FB, FN) binding to $\alpha_v\beta_3$.

Fluid Shear Stress Triggers PKG II, Shp-2, and Src Recruitment to β_3 Integrin-containing Focal Adhesions

Osteoblast stimulation by fluid shear stress induces assembly of actin stress fibers and β_1 integrin-containing focal adhesions (23). We found that fluid shear stress promoted clustering of β_3 with Shp-2 in the periphery of osteoblasts (fig. S6), and increased Shp-2/β_3 coimmunoprecipitation (fig. S7A). Similarly, Kapur et al. reported that Shp-1 and Shp-2 association with β_3 is enhanced by fluid shear stress in human osteosarcoma cells (27). Fluid shear stress increased the colocalization of PKG II and Src with Shp-2 in the plasma membrane (fig. S6), and the amount of PKG II associated with a detergent-insoluble fraction containing cytoskeletal and focal adhesion proteins (Fig. 6, A and B); there was no change in the amounts of β-actin or caveolin-1 associated with the detergent-insoluble fraction, but there was a trend towards increased vinculin, which did not reach statistical significance. With vinculin serving as a focal adhesion marker, triple immunofluorescence staining showed the percentage of focal adhesions containing PKG II and Shp-2, or Src and Shp-2, increased from ~20% in static cells to ~40% in shear-stressed osteoblasts (Fig. 6, C and D). We also assessed the association of PKG II with β_3-containing integrins by bimolecular fluorescence complementation (BiFC). Two chimeras were co-transfected with human β_3

into MC3T3 cells: PKG II-VN containing the N-terminal half of the Venus fluorophore fused between the N-terminal membrane localization signal and the leucine zipper of PKG II, and α_{IIb}-VC containing the C-terminal half of Venus fused to the C-terminus of human α_{IIb} (Fig. 6E). We observed Venus fluorescence in the periphery of cells co-expressing α_{IIb}-VC/β3 with wild-type PKG II-VN, but not with mutant PKG II(G2A)-VN missing the N-terminal myristoylation signal; this suggests interactions between membrane-bound PKG II and α_{IIb}/β3, either direct or indirect (Fig. 6E and fig. S7B, which shows expression of the transfected proteins). We also demonstrated interactions between PKG II, β_3, Shp-2, and Src in reciprocal coimmunoprecipitation experiments (fig. S7C). Based on these data and the fact that Shp-1 and -2 co-immunoprecipitate (Fig. 4H), we conclude that PKG II, β_3, Src, and Shp-1/2 may be present in a large complex, and that fluid shear stress promotes assembly of this complex at focal adhesions. Since β_3 integrin-containing focal adhesion complexes have been implicated as mechanosensors in osteoblasts and osteocytes and other cells (28,29), we propose that this PKG II-, β_3- Src-, and Shp-1/2-containing complex represents a mechanosome modulated by PKG II. The term “mechanosome” was previously coined to describe a hypothetical signaling complex composed of focal adhesion-associated proteins assembled and activated by mechanical stimulation (30).

Src/Erk Signaling is Impaired in Osteoblasts from PKG II-null Mice

PKG II-deficient mice exhibit abnormalities in chondroblast differentiation, but osteoblasts were not previously examined (13). Primary osteoblasts from calvariae of PKG II−/− mice and their wild-type litter mates were morphologically similar; as expected, PKG II−/− osteoblasts lacked PKG II mRNA expression, but PKG I mRNA was present in normal quantities (Fig 7A). Src activation in response to fluid shear stress or cGMP was impaired in PKG II−/− osteoblasts, while cells from wild-type litter mates showed robust Src Tyr^{418} auto-phosphorylation and $pTyr^{529}$ dephosphorylation (Fig. 7, B and C). A similarly dramatic difference was seen in fluid shear stress- or cGMP-induced Erk phosphorylation. Since *fos* family genes are targets of PKG II and Erk (5), we assessed the effect of NO/cGMP/PKG II signaling in one week-old mice by measuring *c-fos* and *fra-2* mRNA expression in tibial diaphyses. The amount of *c-fos* and *fra-2* transcripts was significantly lower in the tibial shafts of PKG II−/− mice compared to wild-type mice, with glyceraldehyde-3-phosphate dehydrogenase mRNA showing no difference and serving as an internal control (Fig. 7D). These results indicate that PKG II deficiency affects *c-fos* and *fra-2* expression in bones of intact animals. Fos family transcription factors play a key role in skeletal development and maintenance (31).

DISCUSSION

We have identified a new mechano-sensitive signaling system in osteoblasts, defining the events leading from shear stress activation of eNOS to Src activation. β_3 integrins function as mechanosensors (28), and the cytoplasmic tail of β_3 serves as a scaffold for a signaling complex that includes Src and Shp-1/2 (26,32,27). We discovered that PKG II is recruited to the β_3-Shp-Src complex in shear-stressed osteoblasts, and that PKG II activated by NO/cGMP phosphorylates and thereby activates Shp-1; the latter dephosphorylates and activates Src (Fig. 7E). Activated Src phosphorylates and recruits the adaptor Shc, which leads to activation of Ras and the Raf/MEK/Erk pathway and stimulation of cell growth (33,34). This signaling system fills a gap in our understanding of how mechanical forces sensed by cell-matrix adhesions are translated into cellular responses, e.g., osteoblast proliferation and osteocyte survival (25). Other mechanisms of Erk activation in shear-stressed osteoblasts include calcium- and focal adhesion kinase-dependent pathways (5,35).

PKG II and Integrins Converge on the Src/Erk Pathway

Current models for mechano-transduction propose that cells sense and respond to forces at their points of attachment to the extracellular matrix, i.e. at integrin-containing focal adhesion complexes (36). Osteocytes are tethered to the canalicular wall via α_v/β_3 integrins (28). In response to mechanical stimulation, integrins cluster and initiate "outside-in" signaling, but the exact nature of force-induced conformational changes in integrins and integrin-associated proteins remain unclear (2,36).

Consistent with reports in other cell types (26,37), we found that Src was associated with the cytoplasmic tail of β_3 integrins, and this association was necessary for Src activation by cGMP/PKG II. Clustering of $\alpha_v\beta_3$ in response to adhesive ligand binding (and/or shear stress) may juxtapose Src molecules and allow partial activation through *trans*-autophosphorylation, but full Src activation downstream of integrins requires action of a protein tyrosine phosphatase, such as PTP-1B in platelets and RPTP-α in fibroblasts (20). We show that Shp-1 and -2, as part of a larger complex, are necessary for fluid shear stress- and cGMP-induced Src activation. Consistent with our finding that Src/Erk activation by the cGMP/PKG II pathway required ligand binding to β_3 integrins, others found that Erk activation by fluid shear stress is prevented by integrin β_3 function-blocking antibodies (24). Some colocalization of Shp-2, Src, and PKG II with β_3-containing complexes was apparent in the plasma membrane of static osteoblasts, but fluid shear stress markedly increased Shp-2, Src, and PKG II recruitment to focal adhesions. In contrast, NO/cGMP activation of PKG induces disassembly of focal adhesions in chondroblasts and endothelial cells (38,39).

PKG II Selectively Targets Shp-1/2 to Activate Src/Erk

Src binds to the SH2-domains of Shp-1 and -2 in vitro, and is a substrate for both phosphatases (40,34). Shp-1 and -2 serve non-redundant functions in Src and Erk activation, and Shp-2 appears to function as a scaffold, coupling Shp-1 and/or Src to growth factor receptors (22,34). Fibroblasts from Shp-2-deficient mice show defective Src and Erk activation in response to integrin ligation and growth factor stimulation (41), and Shp-1-deficient mice develop osteopenia due to combined effects of decreased bone formation and increased resorption (42).

We found that Shp-1 and -2 associate, and that Shp-2 binding to β_3 integrins is increased by fluid shear stress. The Shp-1/2 complex may bind to β3 indirectly, via Shp-2 binding to the Tyr-phosphorylated adaptor protein DOK-1 (32). Shp-1 and -2 are auto-inhibited by interaction between their SH2 and PTP domains, but interaction of the SH2 domains with other Tyr-phosphorylated proteins results in partial phosphatase activation (21). We found that PKG II activation of Shp-1 is mediated by phosphorylation of Ser^{553}, Ser^{556}, and/or Ser^{557} in the C-terminus of Shp-1; in contrast, protein kinase C phosphorylates Shp-1 on Ser^{591} and appears to inhibit phosphatase activity, although reports are conflicting (21). Tyr phosphorylation of Shp-1 and -2 increases phosphatase activity (21), but we found no effect of cGMP/PKGII activation on the phospho-Tyr content of Shp-1/2.

Our results suggest that the main mechanism of PKG II activation of Src is through Shp-1/2-mediated Src $pTyr^{529}$ dephosphorylation, but additional mechanisms could exist, i.e., Src activation by interaction with other SH2- or SH3-domain binding proteins or displacement of C-terminal Src kinase (17). We did not find evidence for direct Src activation by PKG II, in contrast to Src activation by PKA (19). While this manuscript was in preparation, Leung et al. reported that Src activity in ovarian cancer cells depends on basal activity of PKG Iα, with reciprocal phosphorylation between Src and PKG Iα (43). We found no role of PKG I in Src activation in osteoblasts.

PKG II-deficient Mice Have Skeletal Defects

PKG II-deficient mice have no general metabolic disturbances and appear grossly normal at birth, but develop dwarfism because of abnormal endochondral ossification from defective chondroblast differentiation (13). In chondroblasts, PKG II promotes differentiation through regulation of Sox9 and β-catenin (12), and antagonizes growth factor activation of the Raf-1/MEK/Erk cascade (44); this is in contrast to our findings in osteoblasts and osteocytes.

We found defective Src/Erk signaling in PKG II-deficient primary osteoblasts and decreased amounts of *c-fos* and *fra-2* mRNA in tibial diaphyses of PKG−/− mice *versus* wild-type litter mates. Since *c-fos* and *fra-2* are PKG II target genes, these data suggest that *c-fos* and *fra-2* mRNA abundance is regulated by PKG II activity in vivo. *c-fos* is involved in osteoblast cell cycle regulation (45), and mechanical loading-induced *c-fos* expression in bone correlates with new bone formation (7). Since the global PKG II knockout phenotype is dominated by impaired endochondral ossification leading to abnormal architecture of long bones and vertebrae, we plan to generate osteoblast and osteocyte-specific PKG II knockout mice to fully evaluate in vivo consequences of defective osteoblast mechanotransduction.

NO/cGMP/PKG II Signaling is Important for Osteoblast Mechanotransduction

Skeletal maintenance requires continuous mechanical input, as evidenced by bone mass loss in unloaded limbs due to decreased osteoblastic bone formation and increased osteoclastic resorption (1,2). NO is crucial to the anabolic response to mechanical stimulation in vivo: (i) in models of bone adaptation to loading, NOS inhibitors prevent loading-induced c-*fos* mRNA expression and impede osteogenesis (7,11); and (ii) in a hind limb suspension model, eNOS- or iNOS-deficient mice exhibit the same bone loss in unloaded limbs as wild-type mice, but the eNOS−/− mice are not protected from bone loss by venous ligation-induced fluid shear, and the iNOS−/− mice show impaired re-loading osteogenesis (10,6).

We have identified a new link between mechanical stimulation and Src/Erk activation, establishing a central role of NO/cGMP/PKG II signaling in osteoblast mechanotransduction. Pre-clinical and clinical studies support osteogenic functions of NO, although optimal dosing of NO and the potential for NO-induced oxidative stress may be problematic (46). Our results suggest that cGMP-elevating agents such as NO-independent soluble guanylate cyclase activators and phosphodiesterase inhibitors could have favorable “mechano-mimetic” effects on bone.

MATERIALS AND METHODS

Reagents and DNA constructs

Sources of reagents, including antibodies, siRNAs, plasmid and viral vectors are described in Supplementary Materials.

Cell Culture, Transfections, and Exposure to Drugs and Fluid Shear Stress

MC3T3-E1 transformed murine osteoblast-like cells (from the ATCC, used at <12 passages) and hPOBs (established from surgical specimens according to an institutionally-approved protocol) were cultured, transfected with Lipofectamine 2000™ (InVitrogen), and characterized by histochemical staining for alkaline phosphatase and osteocalcin mRNA expression as described (5). Cells were plated on etched glass slides, serum deprived (in 0.1% fetal bovine serum) for 24 hours, and exposed to laminar fluid shear stress (12 dynes/cm^2) in a parallel-plate flow chamber (Cytodyne Inc., San Diego, CA) for 5 min unless noted otherwise. Sham-treated cells were grown under identical conditions and were placed in the flow chamber, but not subjected to shear stress. Serum-deprived cells were pre-incubated with pharmacological inhibitors for 1 hour, and treated with 100 μM 8-(4-

chlorophenylthio)-guanosine-3′,5′-cyclic monophosphate (8-CPT-cGMP, referred to as cGMP) for 5 min unless noted otherwise.

Cell Fractionation, Immunoprecipitation, and Immunoblotting

Detailed protocols for generation of membrane and cytosolic fractions, preparation of detergent-insoluble fractions containing focal adhesion proteins, immunoprecipitations, and Western blotting are provided in Supplementary Materials.

Phosphorylation Assays

Recombinant Shp-1 and Shp-2 were purified from bacteria as glutathione-S-transferase (GST)-fusion proteins bound to glutathione sepharose; proteins were incubated for 15 min at 37°C in the presence of 10 μM [γ-$^{32}PO_4$]ATP, 10 μM cGMP, 10 mM $MgCl_2$, and 50 ng of Flag-tagged PKG II (purified from 293T cells). To examine Shp-1 phosphorylation in intact cells, 293T cells were transfected with Flag-tagged Shp-1 constructs and incubated with $^{32}PO_4$ (100 μCi/ml) for 4 hours, with 100 μM 8-CPT-cGMP added for the last 10 min. Cell lysates were subjected to immunoprecipitation with anti-Flag antibody, and immunoprecipitates were analyzed by SDS-PAGE/autoradiography.

PTP Assays

Variable amounts of GST-Shp-1 constructs purified from bacteria, Flag-Shp-1 constructs immunoprecipitated from transfected 293T cells, and anti-Shp-2 immunoprecipitates from MC3T3 cells were incubated for 15–60 min at 37°C with 100 μM of C-terminal Src peptide [TSTEPQ(pY)QPGENL, from AnaSpec]. Inorganic phosphate was measured by a colorimetric assay in a 96 well plate reader using malachite green/ammonium molybdate; the assay was linear with time and protein concentration.

Immunofluorescence Staining, BrdU Incorporation, and BiFC

Osteoblasts were either exposed to laminar fluid shear stress as described above, or were plated on glass cover slips in 24 well dishes and subjected to orbital fluid shear stress (120 rpm) for 5 min with similar results (Fig. 6 and fig. S6 show orbital fluid shear stress). A detailed description of BrdU treatment, transfection for BiFC, and sample preparation is provided in Supplementary Materials. Cells were viewed with a confocal microscope (Olympus FV1000), a 40/1.3 oil-immersion objective, and 2–4 × digital zoom. Images were analyzed with Fluoview (Olympus) and Photoshop (Adobe), and identical software settings were used for image acquisition of all samples in a given experiment.

Reverse Transcription - Polymerase Chain Reaction (RT-PCR)

RNA was extracted in Tri-Reagent™, and 1 μg of total RNA was subjected to reverse transcription and real-time PCR using previously described primers; *gapd* served as an internal reference using the $2^{-\Delta\Delta Ct}$ method (5).

PKG II −/− mice

Homozygous PKG II knockout mice were generated as described (13); mice from each litter were genotyped by PCR, and tissues were harvested at the University of Bonn, Germany, with approval of the local Animal Welfare Committee. Osteoblast-like cells were extracted from the calvariae of 7 d old mice by sequential collagenase digestion, and cells were characterized as described for hPOBs.

Statistical Analyses

Pair-wise comparisons were done by two-tailed Student's t test, and comparison of multiple groups by ANOVA, with a Dunnett's post-test analysis to the control group; a p value of < 0.05 was considered statistically significant. The Wilcoxon Rank Test was used for results of immunofluorescence staining.

Supplementary Material

Refer to Web version on PubMed Central for supplementary material.

Acknowledgments

We are grateful to T. Diep, A. Fridman, and J. Meerloo for technical support, to S. Ball, G. Firestein, and D. Boyle for providing operative bone specimens.

Funding: This work was supported by NIH grants R01AR051300 (to R.B.P), T32HL007261 (N.M.), and P30NS047101 (UCSD Neuroscience Microscopy Shared Facility).

References

1. Ozcivici E, Luu YK, Adler B, Qin YX, Rubin J, Judex S, Rubin CT. Mechanical signals as anabolic agents in bone. Nat Rev Rheumatol. 2010; 6:50–59. [PubMed: 20046206]
2. Bikle DD. Integrins, insulin like growth factors, and the skeletal response to load. Osteoporos Int. 2008; 19:1237–1246. [PubMed: 18373051]
3. Papachroni KK, Karatzas DN, Papavassiliou KA, Basdra EK, Papavassiliou AG. Mechanotransduction in osteoblast regulation and bone disease. Trends Mol Med. 2009; 15:208–216. [PubMed: 19362057]
4. McAllister TN, Frangos JA. Steady and transient fluid shear stress stimulate NO release in osteoblasts through distinct biochemical pathways. J Bone Miner Res. 1999; 14:930–936. [PubMed: 10352101]
5. Rangaswami H, Marathe N, Zhuang S, Chen Y, Yeh JC, Frangos JA, Boss GR, Pilz RB. Type II cGMP-dependent protein kinase mediates osteoblast mechanotransduction. J Biol Chem. 2009; 284:14796–14808. [PubMed: 19282289]
6. Watanuki M, Sakai A, Sakata T, Tsurukami H, Miwa M, Uchida Y, Watanabe K, Ikeda K, Nakamura T. Role of inducible nitric oxide synthase in skeletal adaptation to acute increases in mechanical loading. J Bone Miner Res. 2002; 17:1015–1025. [PubMed: 12054156]
7. Chow JW, Fox SW, Lean JM, Chambers TJ. Role of nitric oxide and prostaglandins in mechanically induced bone formation. J Bone Miner Res. 1998; 13:1039–1044. [PubMed: 9626636]
8. Mancini L, Moradi-Bidhendi N, Becherini L, Martineti V, MacIntyre I. The biphasic effects of nitric oxide in primary rat osteoblasts are cGMP dependent. Biochem Biophys Res Commun. 2000; 274:477–481. [PubMed: 10913363]
9. Armour KE, Armour KJ, Gallagher ME, Godecke A, Helfrich MH, Reid DM, Ralston SH. Defective bone formation and anabolic response to exogenous estrogen in mice with targeted disruption of endothelial nitric oxide synthase. Endocrinology. 2001; 142:760–766. [PubMed: 11159848]
10. Bergula AP, Haidekker MA, Huang W, Stevens HY, Frangos JA. Venous ligation-mediated bone adaptation is NOS III-dependent. Bone. 2004; 34:562–569. [PubMed: 15003804]
11. Turner CH, Takano Y, Owan I, Murrell GA. Nitric oxide inhibitor L-NAME suppresses mechanically induced bone formation in rats. Am J Physiol. 1996; 270:E634–E639. [PubMed: 8928770]
12. Hofmann F, Bernhard D, Lukowski R, Weinmeister P. cGMP regulated protein kinases (cGK). Handb Exp Pharmacol. 2009:137–162. [PubMed: 19089329]

13. Pfeifer A, Aszòdi A, Seidler U, Ruth P, Hofmann F, Fässler R. Intestinal secretory defects and dwarfism in mice lacking cGMP-dependent protein kinase II. Science. 1996; 274:2082–2086. [PubMed: 8953039]

14. Kapur S, Baylink DJ, Lau KH. Fluid flow shear stress stimulates human osteoblast proliferation and differentiation through multiple interacting and competing signal transduction pathways. Bone. 2003; 32:241–251. [PubMed: 12667551]

15. Jiang GL, White CR, Stevens HY, Frangos JA. Temporal gradients in shear stimulate osteoblastic proliferation via ERK1/2 and retinoblastoma protein. Am J Physiol. 2002; 283:E383–E389.

16. Lau KH, Kapur S, Kesavan C, Baylink DJ. Up-regulation of the Wnt, estrogen receptor, insulin-like growth factor-I, and bone morphogenetic protein pathways in C57BL/6J osteoblasts as opposed to C3H/HeJ osteoblasts in part contributes to the differential anabolic response to fluid shear. J Biol Chem. 2006; 281:9576–9588. [PubMed: 16461770]

17. Harrison SC. Variation on an Src-like theme. Cell. 2003; 112:737–740. [PubMed: 12654240]

18. Gudi T, Hong GKP, Vaandrager AB, Lohmann SM, Pilz RB. Nitric oxide and cGMP regulate gene expression in neuronal and glial cells by activating type II cGMP-dependent protein kinase. FASEB J. 1999; 13:2143–2152. [PubMed: 10593861]

19. Schmitt JM, Stork PJ. PKA phosphorylation of Src mediates cAMP's inhibition of cell growth via Rap1. Mol Cell. 2002; 9:85–94. [PubMed: 11804588]

20. Shattil SJ. Integrins and Src: dynamic duo of adhesion signaling. Trends Cell Biol. 2005; 15:399–403. [PubMed: 16005629]

21. Poole AW, Jones ML. A SHPing tale: perspectives on the regulation of SHP-1 and SHP-2 tyrosine phosphatases by the C-terminal tail. Cell Signal. 2005; 17:1323–1332. [PubMed: 16084691]

22. Wang N, Li Z, Ding R, Frank GD, Senbonmatsu T, Landon EJ, Inagami T, Zhao ZJ. Antagonism or synergism. Role of tyrosine phosphatases SHP-1 and SHP-2 in growth factor signaling. J Biol Chem. 2006; 281:21878–21883. [PubMed: 16762922]

23. Pavalko FM, Chen NX, Turner CH, Burr DB, Atkinson S, Hsieh YF, Qiu J, Duncan RL. Fluid shear-induced mechanical signaling in MC3T3-E1 osteoblasts requires cytoskeleton-integrin interactions. Am J Physiol. 1998; 275:C1591–C1601. [PubMed: 9843721]

24. Lee DY, Yeh CR, Chang SF, Lee PL, Chien S, Cheng CK, Chiu JJ. Integrin-mediated expression of bone formation-related genes in osteoblast-like cells in response to fluid shear stress: roles of extracellular matrix, Shc, and mitogen-activated protein kinase. J Bone Miner Res. 2008; 23:1140–1149. [PubMed: 18333755]

25. Plotkin LI, Mathov I, Aguirre JI, Parfitt AM, Manolagas SC, Bellido T. Mechanical stimulation prevents osteocyte apoptosis: requirement of integrins, Src kinases, and ERKs. Am J Physiol. 2005; 289:C633–C643.

26. Arias-Salgado EG, Lizano S, Sarkar S, Brugge JS, Ginsberg MH, Shattil SJ. Src kinase activation by direct interaction with the integrin b cytoplasmic domain. Proc Natl Acad Sci USA. 2003; 100:13298–13302. [PubMed: 14593208]

27. Kapur S, Mohan S, Baylink DJ, Lau KH. Fluid shear stress synergizes with insulin-like growth factor-I (IGF-I) on osteoblast proliferation through integrin-dependent activation of IGF-I mitogenic signaling pathway. J Biol Chem. 2005; 280:20163–20170. [PubMed: 15778506]

28. Wang Y, McNamara LM, Schaffler MB, Weinbaum S. A model for the role of integrins in flow induced mechanotransduction in osteocytes. Proc Natl Acad Sci USA. 2007; 104:15941–15946. [PubMed: 17895377]

29. Geiger B, Spatz JP, Bershadsky AD. Environmental sensing through focal adhesions. Nat Rev Mol Cell Biol. 2009; 10:21–33. [PubMed: 19197329]

30. Pavalko FM, Norvell SM, Burr DB, Turner CH, Duncan RL, Bidwell JP. A model for mechanotransduction in bone cells: the load-bearing mechanosomes. J Cell Biochem. 2003; 88:104–112. [PubMed: 12461779]

31. Wagner EF, Eferl R. Fos/AP-1 proteins in bone and the immune system. Immunol Rev. 2005; 208:126–140. [PubMed: 16313345]

32. Ling Y, Maile LA, Badley-Clarke J, Clemmons DR. DOK1 mediates SHP-2 binding to the alphaVbeta3 integrin and thereby regulates insulin-like growth factor I signaling in cultured vascular smooth muscle cells. J Biol Chem. 2005; 280:3151–3158. [PubMed: 15546884]

33. Chen KD, Li YS, Kim M, Li S, Yuan S, Chien S, Shyy JY. Mechanotransduction in response to shear stress. Roles of receptor tyrosine kinases, integrins, and Shc. J Biol Chem. 1999; 274:18393–18400. [PubMed: 10373445]
34. Lieskovska J, Ling Y, Badley-Clarke J, Clemmons DR. The role of Src kinase in insulin-like growth factor-dependent mitogenic signaling in vascular smooth muscle cells. J Biol Chem. 2006; 281:25041–25053. [PubMed: 16825188]
35. Young SR, Gerard-O'Riley R, Kim JB, Pavalko FM. Focal adhesion kinase is important for fluid shear stress-induced mechanotransduction in osteoblasts. J Bone Miner Res. 2009; 24:411–424. [PubMed: 19016591]
36. Schwartz MA. Cell biology. The force is with us. Science. 2009; 323:588–589. [PubMed: 19179515]
37. Felsenfeld DP, Schwartzberg PL, Venegas A, Tse R, Sheetz MP. Selective regulation of integrin--cytoskeleton interactions by the tyrosine kinase Src. Nat Cell Biol. 1999; 1:200–206. [PubMed: 10559917]
38. Clancy RM, Rediske J, Tang X, Nijher N, Frenkel S, Philips M, Abramson SB. Outside-in signalling in the chondrocyte. J Clin Invest. 1997; 100:1789–1796. [PubMed: 9312179]
39. Smolenski A, Poller W, Walter U, Lohmann SM. Regulation of human endothelial cell focal adhesion sites and migration by cGMP-dependent protein kinse I. J Biol Chem. 2000; 275:25723–25732. [PubMed: 10851246]
40. Somani AK, Bignon JS, Mills GB, Siminovitch KA, Branch DR. Src kinase activity is regulated by the SHP-1 protein-tyrosine phosphatase. J Biol Chem. 1997; 272:21113–21119. [PubMed: 9261115]
41. Zhang SQ, Yang W, Kontaridis MI, Bivona TG, Wen G, Araki T, Luo J, Thompson JA, Schraven BL, Philips MR, Neel BG. Shp2 regulates SRC family kinase activity and Ras/Erk activation by controlling Csk recruitment. Mol Cell. 2004; 13:341–355. [PubMed: 14967142]
42. Aoki K, Didomenico E, Sims NA, Mukhopadhyay K, Neff L, Houghton A, Amling M, Levy JB, Horne WC, Baron R. The tyrosine phosphatase SHP-1 is a negative regulator of osteoclastogenesis and osteoclast resorbing activity: increased resorption and osteopenia in me(v)/me(v) mutant mice. Bone. 1999; 25:261–267. [PubMed: 10495129]
43. Leung EL, Wong JC, Johlfs MG, Tsang BK, Fiscus RR. Protein kinase G type Ialpha activity in human ovarian cancer cells significantly contributes to enhanced Src activation and DNA synthesis/cell proliferation. Mol Cancer Res. 2010; 8:578–591. [PubMed: 20371672]
44. Krejci P, Masri B, Fontaine V, Mekikian PB, Weis M, Prats H, Wilcox WR. Interaction of fibroblast growth factor and C-natriuretic peptide signaling in regulation of chondrocyte proliferation and extracellular matrix homeostasis. J Cell Science. 2005; 118:5089–5100. [PubMed: 16234329]
45. Sunters A, Thomas DP, Yeudall WA, Grigoriadis AE. Accelerated cell cycle progression in osteoblasts overexpressing the c-*fos* proto-oncogene: Induction of cyclin A and enhanced CDK2 activity. J Biol Chem. 2004; 279:9882–9891. [PubMed: 14699150]
46. Wimalawansa SJ. Rationale for using nitric oxide donor therapy for prevention of bone loss and treatment of osteoporosis in humans. Ann NY Acad Sci. 2007; 1117:283–297. [PubMed: 18056048]

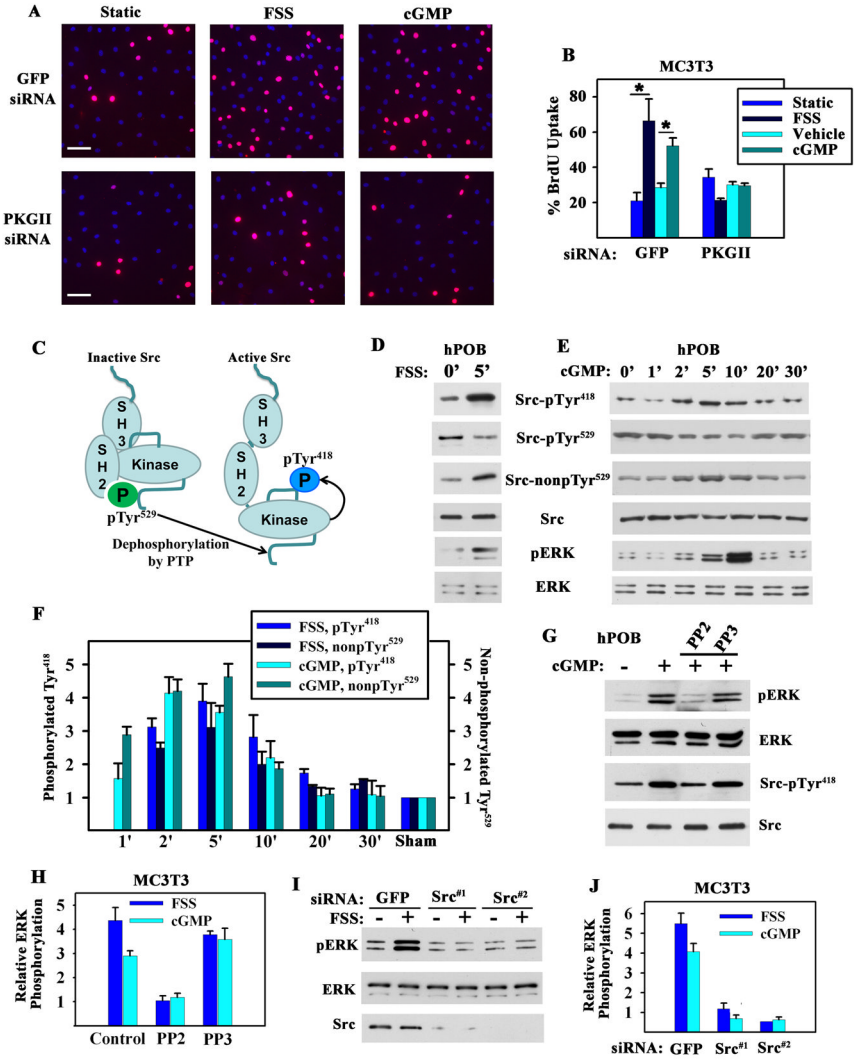

Figure 1. Fluid Shear Stress- and cGMP-induced Osteoblast Proliferation and Erk Activation; Requirements for PKG II and Src

A. and B. MC3T3-E1 transformed murine osteoblast-like cells (MC3T3) were transfected with GFP or PKG II siRNAs, and kept static, exposed to fluid shear stress (FSS; 12 dynes/cm^2), or treated with 100 μM 8-CPT-cGMP (cGMP) for 10 min. BrdU incorporation into DNA was detected by immunofluorescence, with >300 cells analyzed per condition. (B: mean of three experiments ± SEM; *$p < 0.05$).

C. Schema depicting Src activation.

D. and E. hPOBs were sham-treated, subjected to fluid shear stress, or treated with 100 μM cGMP for the indicated times. Western blots were analyzed with phospho-specific antibodies against Src-pTyr^{418}, Src-pTyr^{529}, or Erk-pTyr^{204}, and antibodies recognizing Src with unphosphorylated Tyr^{529}, total Src, or Erk (representative of two experiments).

F. MC3T3 cells were sham-treated, subjected to fluid shear stress, or treated with 100 μM cGMP for the time indicated. Changes in Src phosphorylation were expressed relative to the amount of pTyr^{418} or pTyr^{529} found in sham-treated cells. (mean ± SEM; n=3; $p < 0.05$ for comparison between sham and 2 or 5 min time points).

G. hPOBs were treated with 10 μM PP2 or PP3 for 1 hour and received 100 μM cGMP for 5 min (representative of two experiments).

H. MC3T3 cells were pre-treated with PP2 or PP3 as in G, prior to exposure to either fluid shear stress or 100 μM cGMP for 5 min. Erk phosphorylation was expressed relative to sham-treated cells (mean ± SEM; n=3; *p < 0.05 for the comparison between PP2 *versus* control and PP2 *versus* PP3).

I. and J. MC3T3 cells were transfected with siRNAs targeting GFP or two different sequences in Src, and were exposed to fluid shear stress or treated with 100 μM cGMP for 5 min. (J: mean ± SEM; n=3; *p < 0.05 for the comparison between siRNAs targeting Src *versus* GFP).

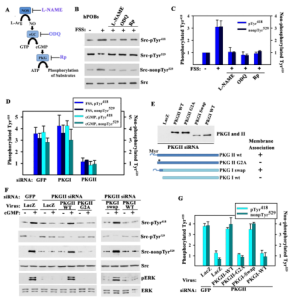

Figure 2. Src Activation by Membrane-bound PKG

A. Schema of the NO/cGMP/PKG signaling pathway with inhibitors of NOS, soluble guanylate cyclase (sGC), and PKG.

B. hPOBs were sham-treated or exposed for 5 min to fluid shear stress (FSS; 12 dynes/cm^2); some cells were pre-treated with 4 mM L-NAME, 10 μM ODQ, or 100 μM Rp-8-CPT-PET-cGMPS (Rp) for 1 hour. Src phosphorylation was determined as in Fig. 1D (representative of two experiments).

C. MC3T3 cells were pre-treated as in B and exposed to fluid shear stress or 100 μM 8-CPT-cGMP (cGMP) for 5 min (mean ± SEM; n=3; * $p < 0.05$ compared to sham).

D. MC3T3 cells were transfected with siRNAs specific for GFP, PKG I or PKG II, exposed to either fluid shear stress or 100 μM cGMP for 5 min, and analyzed as in Fig. 1F (mean ± SEM; n=3; $p< 0.05$ for the comparison between siRNA targeting PKG II *versus* GFP).

E to G. MC3T3 cells were transfected with PKG II (or GFP) siRNA, and infected with adenoviral vectors encoding LacZ (control), siRNA-resistant wild-type (wt) or myristoylation-deficient PKG II (PKG II G2A), and wild-type or membrane-targeted PKG I (PKG I swap). The Western blot in E shows expression of PKG I and II constructs in PKG II siRNA-transfected MC3T3 cells (whole cell lysates); membrane association is indicated as determined by subcellular fractionation. In F, cells were treated with 100 μM cGMP for 5 min or left untreated and cells were analyzed as in Fig. 1E. G shows the mean ± SEM for three experiments ($p < 0.05$ for the comparison of PKG II wt or PKG I swap *versus* LacZ virus in PKG II siRNA-transfected cells).

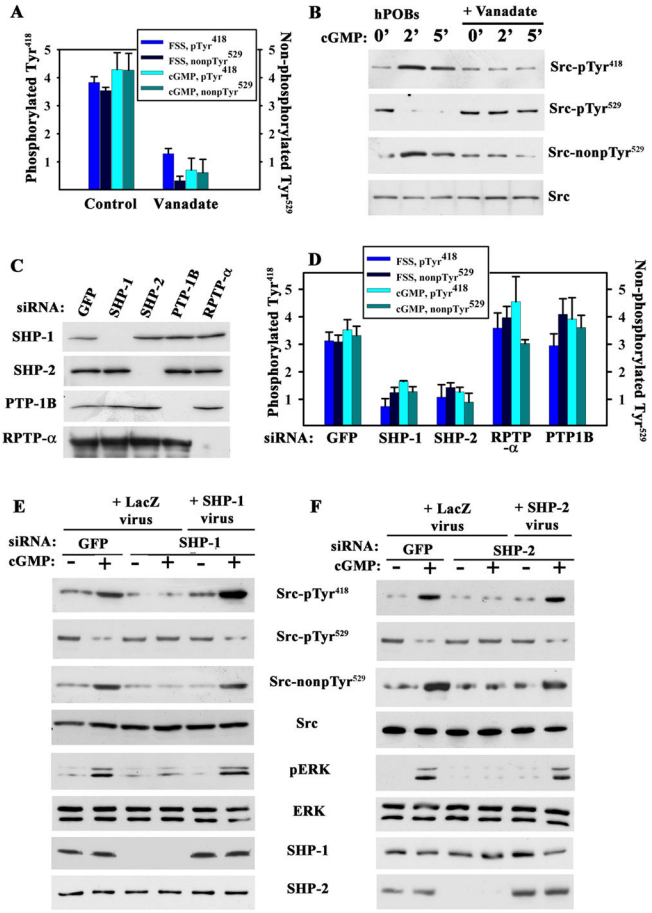

Figure 3. Fluid Shear Stress- and cGMP-induced Src Activation Mediated by Shp-1/2

A. MC3T3 cells were treated with 10 μM vanadate for 1 hour prior to a 5 min exposure to fluid shear stress (FSS; 12 dynes/cm^2) or 100 μM 8-CPT-cGMP (cGMP). Src phosphorylation was analyzed as in Fig. 1F (mean ± SEM; n=3; $p < 0.05$ for vanadate *versus* control).

B. hPOBs were treated with vanadate and cGMP as in A (images are representative of three experiments)

C. and D. MC3T3 cells were transfected with siRNAs targeting GFP, Shp-1, Shp-2, RPTP-α, or PTP-1B, and phosphatase expression was quantified by Western blotting (whole cell lysates for Shp-1, -2, and PTP-1B, and membrane lysates for RPTP-α). In D, cells were exposed to fluid shear stress or treated with 100 μM cGMP for 5 min and Src phosphorylation was analyzed as in Fig. 1F (mean ± SEM; n=3; $p < 0.05$ for the comparison between siRNAs targeting Shp-1 or Shp-2 *versus* GFP).

E. and F. MC3T3 cells were transfected with siRNAs targeting GFP, Shp-1 (E) or Shp-2 (F). Cells were infected with adenovirus encoding LacZ, siRNA-resistant human Shp-1 (E), or Shp-2 (F), and received 100 μM cGMP for 5 min(representative of three experiments).

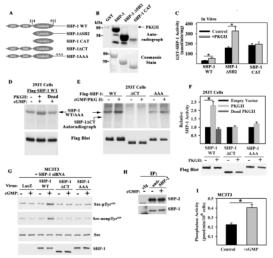

Figure 4. PKG II Phosphorylation of Shp-1/2 and Regulation of PTP Activity

A. Shp-1 constructs; AAA denotes alanine substitutions for Ser^{553}, Ser^{556}, and Ser^{557}.

B. PKG II phosphorylation of bacterially-expressed Shp-1 constructs in the presence of [γ-$^{32}PO_4$]ATP in vitro(representative of three experiments).

C. Effect of PKG II phosphorylation on Shp-1 PTPase activity in vitro (mean ± SEM; n=3; * $p < 0.05$).

D and E. 293T cells were co-transfected with Flag epitope-tagged Shp-1 constructs and empty vector, wild-type PKG II, or kinase-dead PKG II; cells were labeled with $^{32}PO_4$ for 4 hours, and treated with 100 μM 8-CPT-cGMP (cGMP) for 10 min. Immunoprecipitates were analyzed by SDS-PAGE/autoradiography, and protein expression was determined by Western blotting (representative of three experiments). **F. PTP** activity of Flag-tagged Shp-1 constructs immunoprecipitated from 293T cells transfected and treated as in D and E. The activity of each construct was normalized to its activity in PKG-deficient cells (mean ± SEM; n=3; *$p < 0.05$).

G. MC3T3 cells were transfected with Shp-1 siRNA and infected with adenovirus encoding LacZ or siRNA-resistant human Shp-1 wild-type, ΔCT, o**r** AAA. Cells were exposed to 100 μM cGMP for 5 min and Src (de)phosphorylation was analyzed as in Fig. 1E (representative of two experiments).

H. Coimmunoprecipitation of Shp-1 and -2 from MC3T3 cells treated with 100 μM cGMP for 5 min (representative of three experiments).

I. PTP activity in anti-Shp-2 immunoprecipitates (containing Shp-1 and -2) from control MC3T3 cells and from cells treated with 100 μM cGMP for 5 min (mean ± SEM; n=3; *$p < 0.05$).

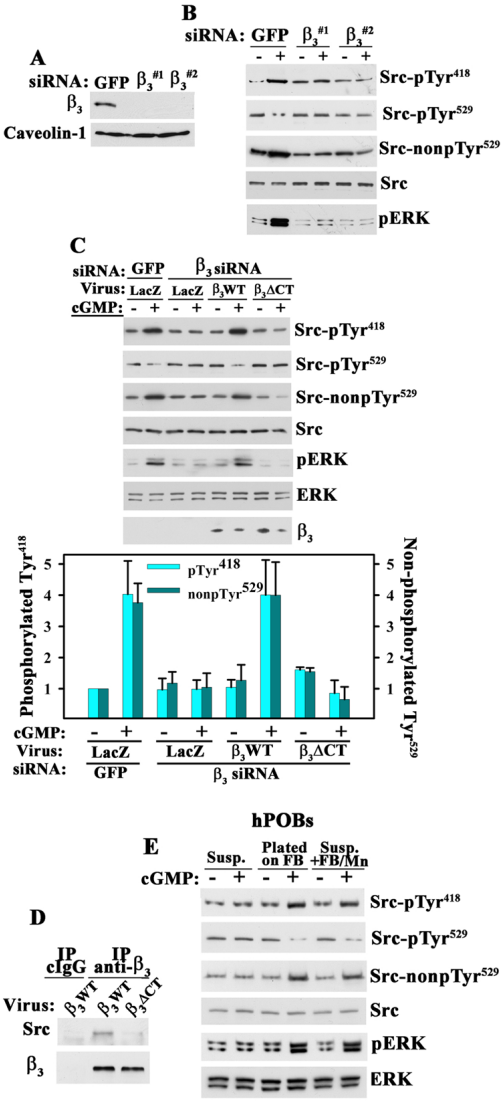

Figure 5. Integrin-dependence of Src Activation by cGMP/PKG II

A. and B. MC3T3 cells were transfected with siRNAs targeting GFP or two different sequences in integrin β_3, and cell membranes were analyzed by Western blotting (A). Cells in B were exposed to 100 μM 8-CPT-cGMP (cGMP) for 5 min and analyzed as in Fig. 1E (representative of three experiments).

C. MC3T3 cells transfected with siRNAs targeting GFP or β_3 were infected with lentivirus encoding siRNA-resistant human β_3WT or Src binding-deficient $\beta_3\Delta$CT. Cells were treated with 100 μM cGMP for 5 min and analyzed as in Fig. 1E. Expression of human β_3 constructs was analyzed by Western blotting of whole cell lysates; the amount of endogenous mouse β_3 is below detection. The bar graph shows the mean ± SEM of three experiments ($p < 0.05$ for β_3WT *versus* LacZ virus in β_3 siRNA-transfected, cGMP-treated cells).

D. Coimmunoprecipitation of Src with wild-type human β_3WT but not $\beta_3\Delta$CT from MC3T3 cells infected with β_3-expressing lentivirus (representative of two experiments). Endogenous murine β_3 is not efficient lt immunoprecipitated. **E.** hPOBs were kept in suspension (Susp.), allowed to attach to fibrinogen (FB)-coated dishes, or kept in suspension and stimulated with soluble fibrinogen (250 μg/ml) plus $MnCl_2$ (2 mM) (Susp.+FB/Mn). After 1 hour,

some cells received 100 μM cGMP for 5 min. Cells were analyzed as in Fig. 1E (representative of three experiments).

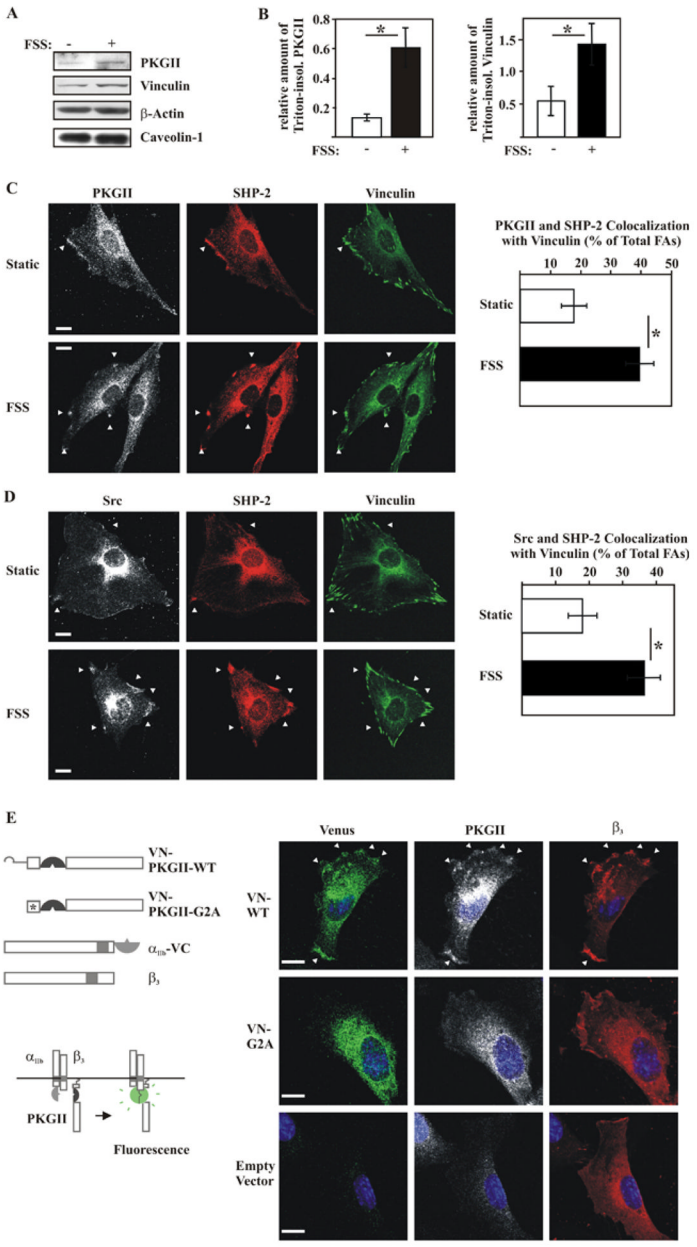

Figure 6. Characterization of a Src-containing Mechano-sensitive Complex in Osteoblasts

A. and B. Western blots of detergent-insoluble fractions isolated from static MC3T3 cells and from cells exposed for 5 min to orbital fluid shear stress (FSS; 120 rpm) (A). The bar graphs in B summarize three separate experiments (mean ± SEM; n=3; *p < 0.05 for static *versus* shear-stressed cells).

C. and D. PKG II (white) and Shp-2 (red), or Src (white) and Shp-2 (red) colocalization with vinculin (green) was examined in static and shear-stressed (FSS) MC3T3 cells (C). Focal adhesions were defined as vinculin-positive membrane complexes > 0.5 μm size, and colocalization of PKG II and Shp-2, or Src and Shp-2 with focal adhesions was scored as a percentage of total focal adhesions (D shows the mean ± standard error of proportion for three experiments, with ~35 cells evaluated per condition; *p < 0.05 for static *versus* shear-stressed cells; bar 5 μm).

D. Colocalization of α_{IIb}/β_3 integrins with PKG II monitored by bimolecular fluorescence complementation (BiFC) between α_{IIb}-VC and wild-type PKG II-VN (VN-WT) or the membrane binding-deficient G2A mutant PKG II-VN (VN-G2A) in MC3T3 cells. All cells were transfected with human β_3 and α_{IIb}-VC (representative confocal images of three separate experiments; bar 5 μm).

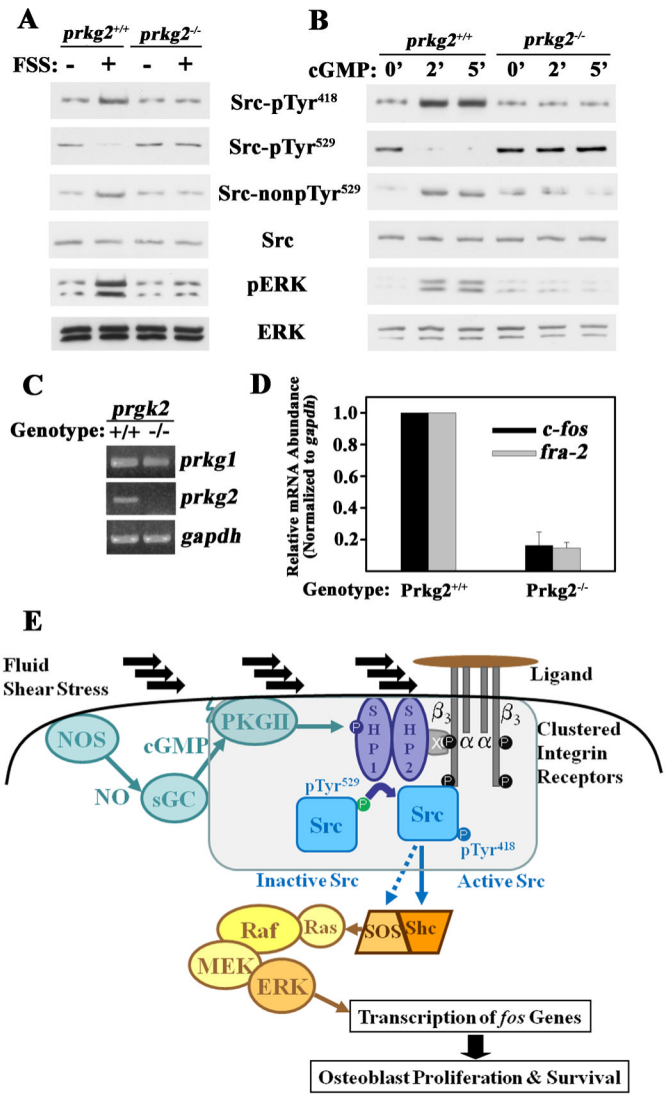

Figure 7. Signaling Defect in PKG II-null Osteoblasts

A. Semi-quantitative RT-PCR for PKG I and II expression in primary calvarial osteoblasts isolated from one week-old PKG II−/− mice and their wild-type litter mates (representative of two experiments).

B. and C. Wild-type and PKG II-null primary osteoblasts were stimulated with either fluid shear stress (FSS; 12 dynes/cm^2) or 100 μM 8-CPT-cGMP (cGMP) for 5 min, and Src and Erk activation were analyzed as in Fig. 1E [representative of two (B) or three (C) experiments].

D. Tibial diaphyses were isolated from one week-old PKG II−/− mice and their wild-type litter mates, and *c-fos*, *fra-2*, and *gapd* mRNA amounts were measured by quantitative RT-PCR (mean ± SEM; n=3; * $p < 0.05$ for wild-type *versus* knockout mice).

E. Model of Src and Erk activation by fluid shear stress via NO/cGMP/PKG II, depicting the assembly of a mechano-sensitive complex containing PKG II, Shp-1/2, and Src bound to the cytoplasmic tail of β_3, as described in the text (x = docking protein). Activation of the Ras/Raf/MEK/Erk cascade by Src occurs via Shc-dependent and -independent pathways (33).